

UV 경화 코팅의 광중합에 대한 라만분광학 분석

Fengguo Liu^{1,2,3,4}, Ying Wang¹, Xiangxin Xue^{1,2,3,4,†}, and He Yang^{1,2,3,4}

¹School of Metallurgy, Northeastern University

²Liaoning Key Laboratory of Metallurgical Resource Recycling Science, Northeastern University

³Liaoning Engineering and Technology Research Center of Boron Resources Comprehensive Utilization, Northeastern University

⁴Liaoning Provincial Universities Key Laboratory of Boron Resources Ecological Utilization Technology and Boron Materials, Northeastern University

(2015년 11월 6일 접수, 2016년 1월 17일 수정, 2016년 2월 19일 채택)

Photopolymerization of UV Curable Coatings Monitored by Raman Spectroscopy

Fengguo Liu^{1,2,3,4}, Ying Wang¹, Xiangxin Xue^{1,2,3,4,†}, and He Yang^{1,2,3,4}

¹School of Metallurgy, Northeastern University, Shenyang 110819, China

²Liaoning Key Laboratory of Metallurgical Resource Recycling Science, Northeastern University, Shenyang 110819, China

³Liaoning Engineering and Technology Research Center of Boron Resources Comprehensive Utilization, Northeastern University, Shenyang 110819, China

⁴Liaoning Provincial Universities Key Laboratory of Boron Resources Ecological Utilization Technology and Boron Materials, Northeastern University, Shenyang 110819, China

(Received November 6, 2015; Revised January 17, 2016; Accepted February 19, 2016)

Abstract: Photopolymerization process of UV curable coatings based on epoxy acrylate/tripropylene glycol diacrylate was monitored by Raman spectroscopy. The consumption of C=C double bond in coatings was observed under UV irradiation. Quantitative analysis of curing degree versus UV irradiation time was investigated by fitting Raman spectra. The results indicated that the initiation efficiency of cleavage type photoinitiators and Irgacure 184 are superior to that of hydrogen-abstraction type photoinitiator. High photoinitiator concentration is beneficial for achieving fast photopolymerization rate and high final conversion. However, when the concentration of photoinitiator exceeds a certain value, the polymerization rate and final conversion will not increase evidently because of initiation efficiency and free volume effect.

Keywords: Raman spectroscopy, UV curable coating, photopolymerization, kinetics.

Introduction

UV curable coatings are regarded as environmentally friendly coatings due to their advantages in energy, ecology, economy, efficiency and enabling (known as 5E).^{1,2} UV curable coatings commonly consist of the multifunctional oligomer, photoinitiator, reactive diluent and other additives. The oligomer is the major composition of film formation under UV radiation. The reactive diluent plays an important role in adjusting the viscosity of the whole coating system, which also participates in the photopolymerization reaction with the oligo-

mer. Photoinitiator is the initial point of curing process. Photoinitiator can absorb UV ray and be decomposed into free radicals or cations with high activity to induce photopolymerization. Other additives including leveling agent, defoamer, matting agent and inorganic filler, act as auxiliaries to improve the properties of coatings. Compared with traditional thermal-curable coatings, UV curable coatings will produce no volatile organic compounds because all constituents are contributed to cured film formation directly or indirectly. As increasing environmental pollution all over the world, UV curable coatings have attracted extensive attention of researchers as a green product with vast potential for further development.³⁻⁵ In recent decade, many researches focused on inorganic-organic composite coating based on UV curing technique for the purposes of improving their properties and expanding applicable range.⁶⁻¹⁰

[†]To whom correspondence should be addressed.

E-mail: xuexx@mail.neu.edu.cn

©2016 The Polymer Society of Korea. All rights reserved.

The curing process of UV curable coatings has a profound influence on its performance. In consequence, it is quite necessary to study the curing behaviour for UV curable coatings. A common technique to study the photopolymerization kinetic is infrared spectroscopy.¹¹⁻¹³ Decker *et al.* reported the application of real-time infrared spectroscopy in polymerization kinetic.¹⁴ Another effective method is photo-DSC technique. It was established based on the quantitative relationship between the reaction heat of polymerization and amount of reacted functional groups.^{15,16} Scott and his co-workers did extremely systematic research on the curing kinetics of vinyl ester resins by photo-DSC.^{17,18} Corcione and his co-workers reported on the cationic photopolymerization of a cycloaliphatic di-epoxy resin in the presence of a hyperbranched OH-terminated polymer.¹⁹ Two complementary techniques, photo-DSC and RT-IR spectroscopy, were used to investigate the photopolymerization reaction at different stages.

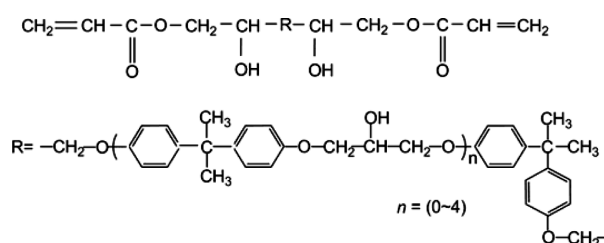
In recent decade, Raman spectroscopy is proved to be a powerful tool to obtain the information of molecular rotation and vibration.²⁰⁻²² The compositions of organic coating including oligomer and reactive diluent contain photosensitive functional groups, which can exhibit corresponding characteristic absorption band in Raman spectra. During the curing process, as the gradual consumption of photosensitive functional groups, the intensity of characteristic absorption bands will decrease accordingly in Raman spectra. Therefore, the curing process can be characterized by monitoring the evolution of characteristic absorption bands. Better resolution of the C=C double bonds can be obtained using Raman spectroscopy, where C=C stretching mode are much stronger than that in IR. Schrof *et al.* reported on the screening effect in UV curable clearcoats using both depth resolved and edge-on Raman microscopy.²³ Posset *et al.* studied the structure-property correlations in hybrid sol-gel coatings by a confocal Raman microscopy.²⁴ Courtecuisse *et al.* studied the oxygen inhibition of acrylate photopolymerization using visible light by confocal Raman microscopy.²⁵ Asmussen *et al.* applied Raman spectroscopy as a tool to monitor the monomer conversions of epoxy and methacrylate hybrid system during photopolymerization.²⁶

In this study, we studied the curing process of UV curable coatings based on epoxy acrylate (EA)/tripropylene glycol diacrylate (TPGDA) using Raman spectroscopy. The influence of the photoinitiator type and concentration on the polymerization rate and conversion was also investigated.

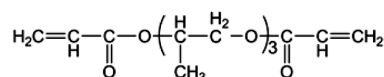
Experimental

Materials. Bisphenol A epoxy acrylate (EA) was purchased from Jiangmen ever-ray Co. Ltd. Tripropylene glycol diacrylate (TPGDA) was purchased from Tianjin Institute of Chemical Reagent. Diphenyl(2,4,6-trimethylbenzoyl)phosphine oxide (TPO), triethanolamine (TEA), 1-hydroxycyclohexyl phenyl ketone (HCPK, Irgacure 184) and benzophenone (BP) were obtained from Sinopharm Chemical Reagent Co. Ltd. All reagents were used as received. The chemical structures of oligomer, reactive diluent and photoinitiators were shown in Figure 1.

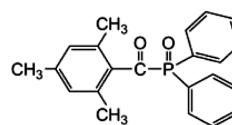
Preparation and Curing of UV Curable Coatings. The UV curable formulations used in this study consisted of EA and TPGDA with a weight rate of 4:5. The photoinitiator was entirely dissolved in EA/TPGDA system by keeping magnetic stirring for 24 h at room temperature. The sample numbers and compositions were listed in Table 1. Hereinto, 0.5 mL of TEA



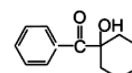
(1) Bisphenol A epoxy acrylate (EA)



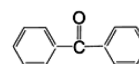
(2) Tripropylene Glycol Diacrylate (TPGDA)



(3) Diphenyl(2,4,6-trimethylbenzoyl)phosphine oxide (TPO)



(4) 1-Hydroxycyclohexyl phenyl ketone (HCPK, Irgacure 184)



(5) Benzophenone (BP)

Figure 1. Chemical structures of oligomer, reactive diluent and photoinitiators.

Table 1. Compositions of UV Curable Coatings

Sample No.	Photoinitiator (wt%)	Sample No.	Photoinitiator (wt%)	Sample No.	Photoinitiator (wt%)
BP-0.5	0.5	TPO-0.5	0.5	184-0.5	0.5
BP-1	1.0	TPO-1	1.0	184-1	1.0
BP-2	2.0	TPO-2	2.0	184-2	2.0
BP-3	3.0	TPO-3	3.0	184-3	3.0
BP-4	4.0	TPO-4	4.0	184-4	4.0

was used as an assistant photoinitiator in BP initiator system.

UV source was obtained from a RW-UVAD301-501y UV curing machine (Shenzhen Runwing Co. Ltd) with a conveyor system. The height of UV source and the belt speed of conveyor were adjusted appropriately. 2 mL of coating sample was placed in a plastic container with 15 mm in diameter. The thickness of resultant cured film was 2.1 mm. The irradiation time of a pass through UV curing machine was 2 s and the UV intensity was 20 mW/cm².

Raman Spectroscopy. Raman spectra were obtained by a HR800 Raman spectrometer (Horiba Jobin Yvon) that utilized a 633 nm HeNe laser with an output power of 9 mW and a 50× objective. For all measurement the slit width was 300 μm and the integral time was 30 s.

Results and Discussion

Raman Spectra Fitting. Raman spectra evolution of UV curable coating based on EA/TPGDA under UV irradiation (3% of BP as photoinitiator) is shown in Figure 2. When the irradiation time is 0 s, the uncured coating is liquid. In the figure, it is easy to observe that the band at 1641 cm⁻¹ is attributed to C=C double bond stretching vibration. The band at 1735 cm⁻¹ is attributed to C=O bond stretching vibration. The bands at 1412 and 1440 cm⁻¹ are attributed to C-H deformation vibration of =CH₂ and -CH₂-, respectively. The Raman intensity is dependent on the species and number of scattering molecules. For a certain Raman band, the intensity is proportional to the concentration of scattering functional group in investigated region. Therefore, we can carry out quantitative analysis by an unaffected band as internal standard. In this study, the consumption of C=C bond increased as increasing the irradiation time. As shown in Raman spectra, the intensity of band at 1641 cm⁻¹ decreased by degrees. Conversely, C=O bond did not participate in the photochemical polymerization and would keep in a constant concentration. C=O bond stretching vibration at 1735 cm⁻¹ was a suitable candidate as internal standard

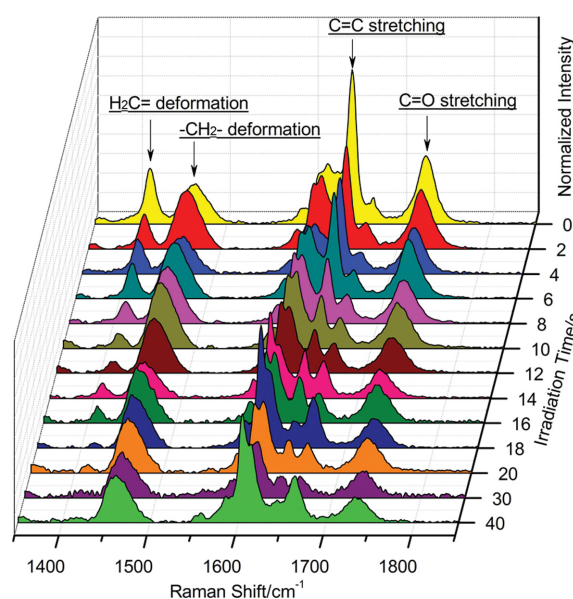


Figure 2. Raman spectra evolution of UV curable coating based on EA/TPGDA under UV irradiation (3% of BP as photoinitiator).

because of its strong intensity. The conversion rate of C=C bond can be calculated by following equation:²⁷

$$\text{Conversion rate} = \left(1 - \frac{I_{C=C,t} \cdot I_{C=O,0}}{I_{C=C,0} \cdot I_{C=O,t}}\right) \times 100\% \quad (1)$$

Where $I_{C=C,0}$, $I_{C=O,0}$ is the intensity of C=C and C=O bond in uncured coatings; $I_{C=C,t}$, $I_{C=O,t}$ is the intensity of C=C and C=O bond at a certain irradiation time.

In general, Gaussian curve and Lorentzian curve are utilized for fitting Raman spectra. The mathematical equations are as follows.^{28,29}

$$\text{Gaussian: } I_G = I_0 \times \exp[-2(x-x_0)^2/(\omega^{1/2})^2] \quad (2)$$

$$\text{Lorentzian: } I_L = I_0 \times \left[\frac{(\omega^{1/2})^2}{(\omega^{1/2})^2 + 4(x-x_0)^2} \right] \quad (3)$$

Where the intensity of any point on the band. I_0 is the maximal intensity of the band. x_0 is Raman shift at the maximal

intensity. x is Raman shift of any point on the band. $\omega_{1/2}$ is the full width at half maximum of Raman band. According to classical electromagnetic field theory, Raman band was proved to be in a shape of Lorentzian function. In practice, the Raman band we obtained from the equipment is the convolution of its natural line shape, instrumental transfer function and disorder-induced distribution of vibrators, which generally can be considered as Gaussian function shape. Bradley stated that the Gaussian profile works well for solid samples, powders, gels or resins.³⁰ The Lorentzian profile works better for gases, but can also fit liquids in many cases. The combined Gaussian and Lorentzian function could obtain more authentic fitting results in some cases. Herein, we use weighted values of Gaussian and Lorentzian function to fit Raman spectra:

$$I_{(L+G)} = f \cdot I_L + (1 - f) \cdot I_G \quad (4)$$

Where f is the weight of Lorentzian curve (f is 0.5 in this study).

Fitting curves of Raman spectra for uncured and cured coatings were shown in Figure 3. There are five other overlapping bands nearby C=C stretching vibration band. We have to fit all the correlative bands in order to obtain the intensity of C=C stretching vibration. Nichols *et al.* reported a smoothed second-derivative processing approach to overcome the difficulties of sample fluorescence and baseline shifts.²⁰ However, overlapping bands would lead to a larger error of fitting results using this method. From Figure 2 we can see that the =CH₂ deformation vibration band at 1412 cm⁻¹ is not overlapped with other bands. From the chemical structures of the oligomer and reactive diluent, we can see that the positions of C=C double

Table 2. Conversions Calculated by Two Bands

	I_{1412} (cm ⁻¹)	I_{1641} (cm ⁻¹)	I_{1735} (cm ⁻¹)
$t = 0$ s	5522.3	14158.6	6271.9
$t = 40$ s	59.9	151.1	247.5
Conversion (%)	72.51	72.96	

bonds in both EA and TPGDA are located at the both ends of molecular chains. The amount in mole of =CH₂ is equal to the amount of C=C double bonds that can participate in the photopolymerization. Thus, Raman intensity of =CH₂ deformation vibration band will decrease in proportion to the consumption of C=C double bonds. Herein, it is theoretically feasible to calculate the conversion using =CH₂ deformation vibration band instead of C=C stretching vibration. The calculated conversions are shown in Table 2. From Table 2, we can see the result is agreement with the discussions above. All the following studies on the calculated C=C conversion are based on the consumption of =CH₂.

Influence of Photoinitiator Type on C=C Double Bond Conversion. As a key component of UV curable coatings, photoinitiator plays an important role in curing process. Free radical photoinitiator can be classified as cleavage type and hydrogen-abstraction type photoinitiator. In this study, TPO and Irgacure 184 are cleavage type photoinitiators. BP is hydrogen-abstraction type photoinitiator. Figure 4 shows the plot of the C=C double bond conversion versus UV irradiation time with three photoinitiators at the same concentration (3% in mass ratio). With TPO and Irgacure 184 as photoinitiator, the conversion of C=C double bond in UV curable coatings can reach 76% and 87% in 2 s, respectively. Contrastively, the

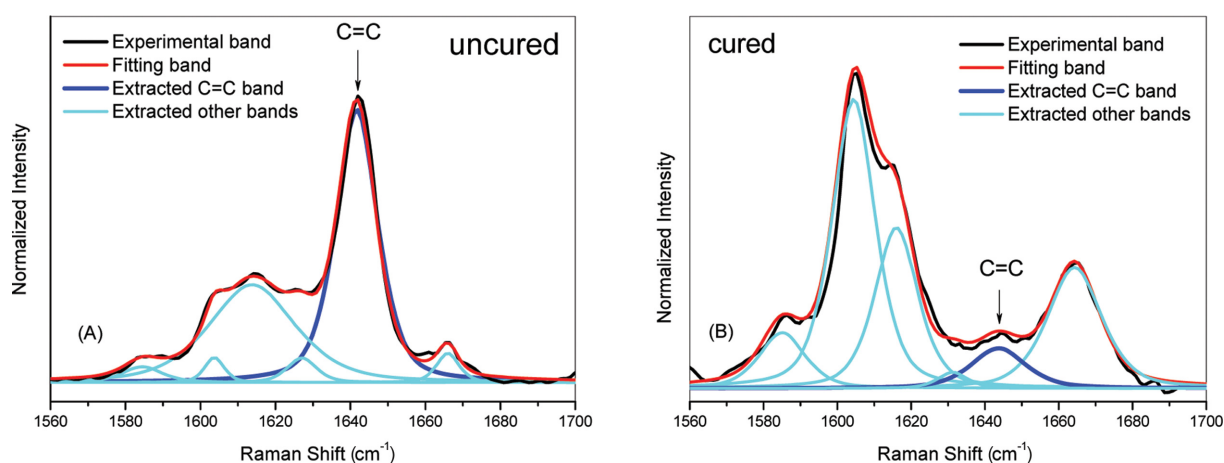


Figure 3. Fitting Raman spectra of uncured (A); cured coatings (B).

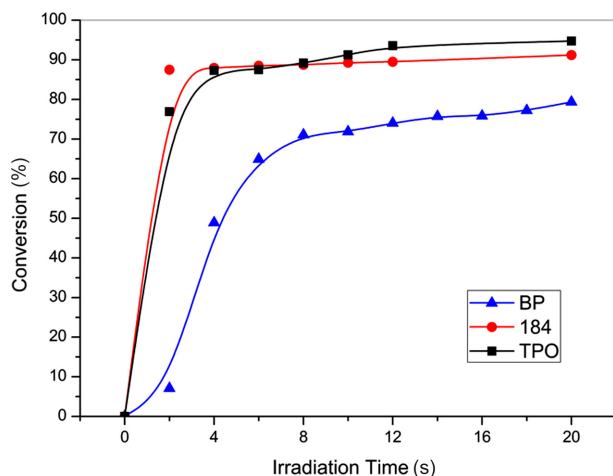


Figure 4. Plot of the C=C double bond conversion *versus* UV irradiation time with three photoinitiators: BP, TPO and Irgacure 184.

conversion only reaches 7% in 2 s with BP as photoinitiator and reaches above 70% after 8 s. It is quite obvious that the initiation rate of cleavage type photoinitiator is much higher than that of hydrogen-abstraction type photoinitiator. The results accord with Decker and his co-worker's investigation.¹⁴ In addition, for the final conversion after 20 s irradiation, it indicated that the effect of TPO (94% of conversion) and Irgacure 184 (91% of conversion) are better than that of BP (79% of conversion).

The photochemical initiation process of TPO, Irgacure 184 and BP is shown in Figure 5. The cleavage type photoinitiator can be decomposed as primary free radical with high activity under UV irradiation. As shown in Figure 5, TPO produces

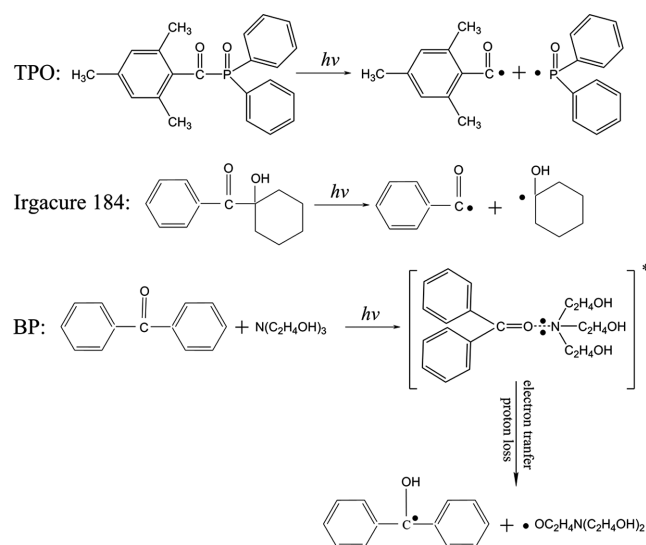


Figure 5. Photochemical initiation of TPO, Irgacure 184, and BP.

trimethylbenzoyl radical and diphenyl phosphinyl radical. Irgacure 184 produces hydroxycyclohexyl radical and benzoyl radical. These free radicals can directly induce polymerization of the oligomer and reactive diluent. As a hydrogen-abstraction type photoinitiator, BP reacts with assistant photoinitiator tertiary amine with α -H (as a hydrogen donor) after UV irradiation and generates an exciplex. Subsequently, the exciplex generates ketyl radical and α -aminoalkyl radical after the process of electron transfer and proton loss. As the ketyl radical is inactive, α -aminoalkyl radical plays a leading role in inducing the polymerization. Precisely because of the different initiation mechanism, the efficiency of cleavage type photoinitiator are superior to that of hydrogen-abstraction type photoinitiator.²

Influence of Photoinitiator Concentration on C=C Double Bond Conversion. The photoinitiator concentration is one of major factors affecting the curing degree of UV curable coatings. The plot of C=C double bond conversion *versus* UV irradiation time with various concentrations of photoinitiators is shown in Figure 6. As shown in Figure 6(A), when TPO concentration is 0.5% in mass ratio, the polymerization rate of coatings is slower and the final C=C double bond conversion is below 70% under UV irradiation for 20 s. When TPO concentration is 1%, the polymerization rate of coatings becomes distinctly faster and the final C=C double bond conversion increases to above 80%. However, no such substantial increase of polymerization rate and final conversion are observed when TPO concentration is increased more than 1%. The similar laws are found in Irgacure 184 and BP as shown in Figure 6(B) and Figure 6(C). The results are consistent with Lecamp and his co-workers' researches.^{31,32} For comprehensive consideration of saving cost and achieving higher curing degree of coatings, we can summarize an optimal photoinitiator concentration in EA/TPGDA system: 1% of TPO, 2% of Irgacure 184 and 3% of BP.

According to the principles of photopolymerization, if the initiation rate is higher than photoinitiator dissociation rate, the rate of photopolymerization can be expressed by the following equation:^{32,33}

$$R_p = -\frac{d[M]}{dt} = \frac{k_p}{k_t^{0.5}} [M]_0 (\Phi \varepsilon I_0 [A]_0)^{0.5} \quad (5)$$

Where k_p and k_t are the propagation and termination rate constants, Φ is the quantum yield, ε is the absorption coefficient, I_0 is the incident light intensity, $[M]_0$ is the molar concentration of the C=C double bond, and $[A]_0$ is the photoinitiator concentration. By the equation, the polymerization

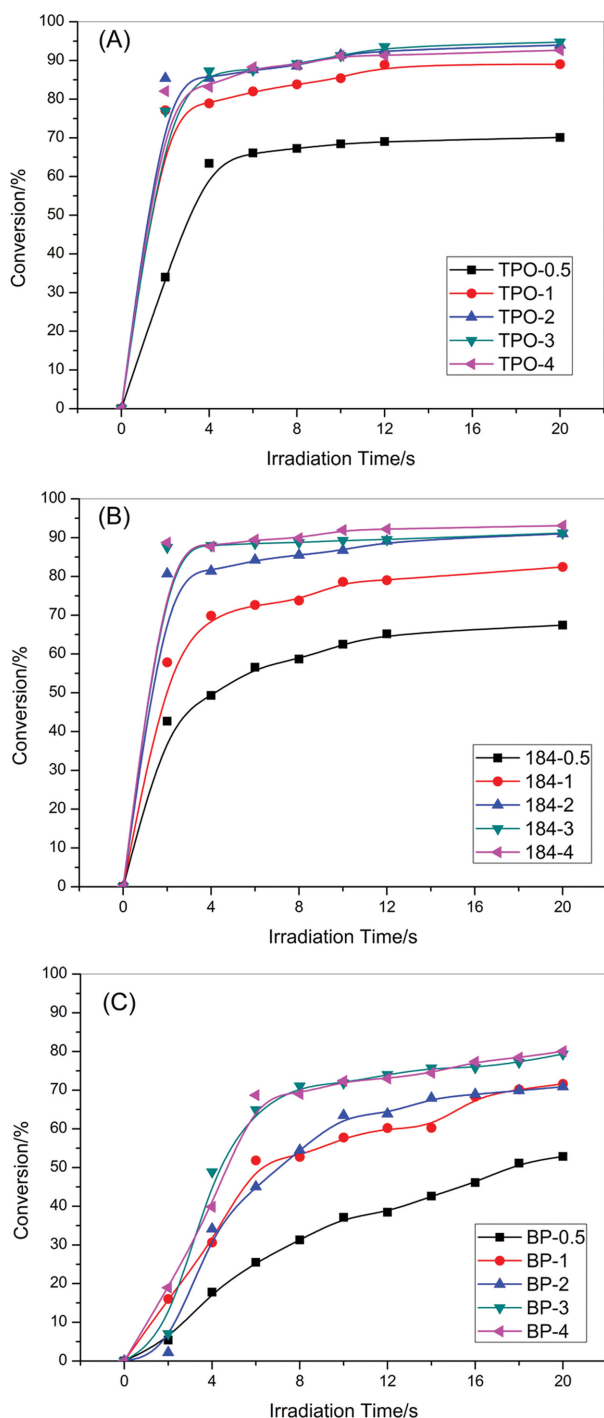


Figure 6. Plot of C=C double bond conversion *versus* UV irradiation time with various concentrations of photoinitiators: (A) TPO; (B) Irgacure 184; (C) BP.

rate is proportional to the 0.5 th power of the photoinitiator concentration. However, the results in this study are not completely consistent with it. When the concentration of photoinitiator exceeds a certain value, the polymerization rate will

not increase at such a ratio.

During the photopolymerization process, the quantum yield of photoinitiator is defined by the ratio of photon number inducing polymerization and photon number absorbed by photoinitiator. Therefore, the more the quantum yield, the faster photopolymerization rate is. Actually, the primary radicals produced by photoinitiator in UV curable system will go through two potential competitive procedures. One is the polymerization initiation. Another is the extinction between two free radicals or termination between a free radical and polymer chain radical. If the photoinitiator concentration is higher, more free radicals will be produced. Meanwhile, the possibility of radical extinction is increased. This leads to decreasing the initiation efficiency of photoinitiator and then influences the polymerization rate not to reach a theoretical results.

In addition, according to the theory of free volume,^{34,35} there are some temporary free volume in UV curable coatings because the volume shrinkage rate of UV curable coatings is far less than polymerization rate during curing process. These free volume can improve the mobility of active molecule chains and then increase the C=C double bond conversion. In other words, the system with faster polymerization rate will produce more free volume, which is benefit to increase the C=C double bond conversion. On the contrary, when the system with excessive concentration of photoinitiator shows no increasing in polymerization rate, the C=C double bond conversion will not increase correspondingly. It is concluded that the effects of photoinitiator concentration on polymerization rate and C=C conversion are in similar law. Therefore, in this study for EA/TPGDA, we can see that the systems with TPO and Irgacure 184 as photoinitiator show higher C=C conversion than systems with BP at the same concentration. For a photoinitiator, the systems with high photoinitiator concentration show higher C=C conversion than the systems with low photoinitiator concentration.

Conclusions

In summary, photopolymerization process of UV curable coatings based on EA /TPGDA was monitored by Raman spectroscopy. It is an effective method to calculate the conversion using $=CH_2$ deformation vibration band instead of C=C stretching vibration in fitting Raman spectra. Quantitative analysis results indicate that the initiation efficiency of cleavage type photoinitiators TPO and Irgacure 184 are superior to that of hydrogen-abstraction type photoinitiator BP. The faster

photopolymerization rate and higher final conversion of UV curable coatings are achieved at higher photoinitiator concentration. However, when the concentration of photoinitiator exceeds a certain value, the polymerization rate and final conversion will not increase evidently because of initiation efficiency and free volume effect. For comprehensive consideration of saving cost and achieving higher curing degree of coatings based on EA/TPGDA, an optimal photoinitiator concentration was summarized: 1% of TPO, 2% of Irgacure 184 and 3% of BP.

Acknowledgments: Authors acknowledge the financial support from the National Natural Science Foundation of China (No.51074053).

References

1. C. Decker, *Macromol. Rapid Commun.*, **23**, 1067 (2002).
2. Y. Yagci, S. Jockusch, and N. J. Turro, *Macromolecules*, **43**, 6245 (2010).
3. X. Zhang, J. Yang, Z. Zeng, L. Huang, Y. Chen, and H. Wang, *Polym. Int.*, **55**, 466 (2006).
4. H. Wang, J. D. Cho, and J. W. Hong, *J. Appl. Polym. Sci.*, **93**, 1473 (2004).
5. J. H. Aerykssen and I. V. Khudyakov, *Ind. Eng. Chem. Res.*, **50**, 1523 (2011).
6. A. Chemtob, D. L. Versace, C. Belon, C. B. Céline, and S. Rigolet, *Macromolecules*, **41**, 7390 (2008).
7. Y. Y. Yu, W. C. Chien, and S. Y. Chen, *Mater. Des.*, **31**, 2061 (2010).
8. S. Zhang, Z. Chen, M. Guo, J. Zhao, and X. Liu, *RSC Adv.*, **4**, 30938 (2014).
9. Y. Wang, F. Liu, and X. Xue, *Prog. Org. Coat.*, **76**, 863 (2013).
10. B. Yu, X. Wang, W. Xing, H. Yang, L. Song, and Y. Hu, *Ind. Eng. Chem. Res.*, **51**, 14629 (2012).
11. V. Jančovičová, M. Mikula, B. Havlínová, and Z. Jakubíková, *Prog. Org. Coat.*, **76**, 432 (2013).
12. F. Li, S. Zhou, B. You, and L. Wu, *J. Appl. Polym. Sci.*, **99**, 1429 (2006).
13. H. D. Paz, A. Chemtob, C. B. Céline, D. L. Nouen, and S. Rigolet, *J. Phys. Chem. B*, **116**, 5260 (2012).
14. C. Decker and K. Moussa, *Macromolecules*, **22**, 4455 (1989).
15. H. D. Hwang, C. H. Park, J. I. Moon, H. J. Kim, and T. Masubuchi, *Prog. Org. Coat.*, **72**, 663 (2011).
16. C. E. Corcione, M. Frigione, A. Maffezzoli, and G. Malucelli, *Eur. Polym. J.*, **44**, 2010 (2008).
17. T. F. Scott, W. D. Cook, and J. S. Forsythe, *Polymer*, **43**, 5839 (2002).
18. T. F. Scott, W. D. Cook, and J. S. Forsythe, *Polymer*, **44**, 671 (2003).
19. C. E. Corcione, G. Malucelli, M. Frigione, and A. Maffezzoli, *Polym. Test.*, **28**, 157 (2009).
20. M. E. Nichols, C. M. Seubert, W. H. Weber, and J. L. Gerlock, *Prog. Org. Coat.*, **43**, 226 (2001).
21. D. Lampakis, P. N. Manoudis, and I. Karapanagiotis, *Prog. Org. Coat.*, **76**, 488 (2013).
22. J. Jin, H. Lim, H. Park, S. S. Kim, K. Song, and K. Tashiro, *Polym. Korea*, **27**, 603 (2003).
23. W. Schrof, E. Beck, R. Koniger, W. Reich, and R. Schwalm, *Prog. Org. Coat.*, **35**, 197 (1999).
24. U. Posset, K. Gigant, G. Schottner, L. Baia, and J. Popp, *Opt. Mater.*, **26**, 173 (2004).
25. F. Courtécuisse, J. Cerezo, C. Croutxe-Barghorn, C. Dietlin, and X. Allonas, *J. Polym. Sci., Part A: Polym. Chem.*, **51**, 635 (2013).
26. S. Asmussen, W. Schroeder, I. dell'Erba, and C. Vallo, *Polym. Test.*, **32**, 1283 (2013).
27. Y. Cai and J. L.P. Jessop, *Polymer*, **47**, 6560 (2006).
28. G. K. Wertheim, M. A. Butler, K. W. West, and D. N. E. Buchanan, *Rev. Sci. Instrum.*, **45**, 1369 (1974).
29. F. C. Tai, S. C. Lee, J. Chen, C. Wei, and S. H. Chang, *J. Raman Spectrosc.*, **40**, 1055 (2009).
30. M. Bradley, *Thermo Fisher Scientific*, U.S.A., Application Note: 50733 (2007).
31. L. Lecamp, B. Youssef, C. Bunel, and P. Lebaudy, *Polymer*, **40**, 1403 (1999).
32. L. Lecamp, B. Youssef, and C. Bunel, *Polymer*, **38**, 6089 (1997).
33. X. S. Jiang, H. J. Xu, and J. Yin, *Polymer*, **45**, 133 (2004).
34. J. Rudnick, P. L. Taylor, M. Litt, and A. J. Hopfinger, *J. Polym. Sci. Polym. Phys. Ed.*, **17**, 311 (1979).
35. H. L. Frisch, D. Klemperer, and T. K. Kwei, *Macromolecules*, **4**, 237 (2002).